Correlation of preexisting diamagnetic defect centers with induced paramagnetic defect centers by ultraviolet or vacuum-ultraviolet photons in high-purity silica glasses

Hiroyuki Nishikawa,* Ryuta Nakamura, and Yoshimichi Ohki
Department of Electrical Engineering, Waseda University, 3-4-1 Ohkubo, Shinjuku-ku, Tokyo 169, Japan

Yoshimasa Hama
Advanced Research Center for Science and Engineering, Waseda University, 3-4-1 Ohkubo, Shinjuku-ku, Tokyo 169, Japan

(Received 9 August 1993)

Electron-spin-resonance (ESR) and vacuum-ultraviolet (vuv) absorption measurements were performed on a series of high-purity silica glasses exposed to 6.4-eV photons, 7.9-eV photons from excimer lasers, and to γ rays. The concentration of defect centers varies from 10^{14} to 10^{16} cm^{-3} depending on the method of material fabrication and photon energy of the irradiating lasers. Variation of the defect species with both the incident-photon energy and manufacturing condition is observed by ESR measurements. E' centers ($\equiv$Si$\cdot$) are observed in all types of silicas. Nonbridging-oxygen hole centers (NBOHC's $\equiv$Si—O$\cdot$) in high-OH silica ([OH]$\approx$1000 ppm) and peroxy radicals (PR's, $\equiv$Si—O—O$\cdot$) in oxygen-surplus silica ([OH]$<$1 ppm) are observed, only when the samples are exposed to 7.9 eV photons. The defect centers observed in γ-irradiated silica are qualitatively in agreement with those in 7.9 eV laser-irradiated silica. The variation of defect species with manufacturing methods indicates that the observed paramagnetic centers are created from preexisting defects. Concentration of the defects induced by either 6.4 or 7.9 eV laser photons is proportional to the square of the pulse energy, indicating that two-photon absorption process dominates in the defect formation. The defect formation process can be understood in terms of the creation of an electron-hole (e-h) pair by two-photon excitation and the subsequent hole trapping or decay of an e-h pair at the site of preexisting defects. Dependence of the induced-defect species on incident-photon energy can be explained by the variation in the energy level of preexisting defects or in the defect formation energy. Results of vuv-absorption measurements reveal the conversion of diamagnetic precursor defects (e.g., $\equiv$Si—Si$\equiv$, $\equiv$Si—O—O—Si$\equiv$, and $\equiv$Si—OH) introduced during the manufacturing process, into paramagnetic defect centers, the E' centers, NBOHC's, and PR's.

I. INTRODUCTION

There have been numerous efforts to understand the basic mechanisms involved in radiation-induced defect formation in silica glasses.[1–3] Electron-spin-resonance (ESR), optical absorption, and photoluminescence measurements have been employed in these studies.[3–5] Following the observation of the E' center by Weeks,[6] thorough ESR investigations on intrinsic defect centers in silica have been made by Griscom and co-workers, on the basis of ^{29}Si and ^{17}O hyperfine structures.[3,4] To date, four intrinsic defect centers have been identified by ESR: E' center ($\equiv$Si$\cdot$), peroxy radical (PR, $\equiv$Si—O—O$\cdot$), nonbridging-oxygen hole center (NBOHC, $\equiv$Si—O$\cdot$),[3,4] and self-trapped holes (STH_1 and STH_2).[7] Here, the symbols "$\equiv$" and "$\cdot$" represent bonds with three separate oxygens and an unpaired spin, respectively. The E' center, PR, and NBOHC are stable at room temperature, while the STH's are observable only after irradiation below 200 K. ESR-inactive species have been mainly studied by optical absorption measurements in the region from ultraviolet (uv) to vacuum-uv (vuv).[8–13] It has been reported that oxygen vacancy ($\equiv$Si—Si$\equiv$), peroxy linkage ($\equiv$Si—O—O—Si$\equiv$), and hydroxyl ($\equiv$Si—OH) exhibit uv and vuv absorption bands at 5.0 eV (Ref. 10) and 7.6 eV (Refs. 9, 11, and 12), at 3.8 eV (Ref. 13) and 7–8 eV (Refs. 8 and 9), and at 7.5–8 eV (Refs. 8 and 9), respectively.

It was reported by Stathis and Kastner[14] that paramagnetic defect centers are observed in silica (band gap $\approx$9 eV) (Ref. 15) exposed to sub-band-gap uv-vuv photons (5.0, 6.4, and 7.9 eV) from excimer lasers. Motivated by a technological application of uv optics for excimer-laser lithography, several studies have been made to elucidate mechanisms involved in the laser-induced defect creation.[8,16–21] Apart from these technological reasons, it is important to understand the process of photon-induced defect creation in solids, not to mention the example of the Staebler-Wronski effect in a-Si:H.[22]

Mechanisms proposed for the laser-induced defect creation in amorphous SiO_2 (a-SiO_2) can be divided into intrinsic and extrinsic processes. The intrinsic mechanism is a radiolytic process wherein an oxygen atom is displaced out of the normal Si—O—Si bond by the nonradiative decay of self-trapped excitons, while the extrinsic one involves ionization or bond rupture at the site of preexisting defects. The intrinsic mechanism proposed by Griscom[1,2] has been supported by the studies of Tsai, Griscom, and Friebele[19,20] using a highly focused ArF-excimer laser (6.4 eV) with photon density two orders of magnitude higher than other studies. The extrinsic mechanism has been reported to be observable in silica when exposed to ArF-excimer-laser photons with moderate pulse energies of 10–100 mJ/cm^2. Imai and co-workers proposed that the E' centers observed in oxygen-deficient type silicas are induced through a two-photon absorption process based on the observation that the concentration of the E' centers is proportional to the square of pulse energies.[8,17,18] The authors have reported that the observed E' center or NBOHC concentration varies widely from 10^{14} to 10^{16} cm^{-3} in a series of silicas containing various preexisting defects.[21] These studies on the extrinsic defect formation process have demonstrated that preexisting defects play a significant role as precursors in the laser-induced defect formation process. However, due to lack of information on the behavior of preexisting defects under laser irradiation, correlation between preexiting defects and paramagnetic defects is still not fully understood.

In this paper, we report the results of ESR and vuv absorption measurements on silica glasses exposed to 6.4 or 7.9 eV laser photons. The defects induced by 6.4 or 7.9 eV laser are compared with those induced by γ rays. We will discuss how laser-induced defect species and their concentrations depend on manufacturing methods and laser photon energy. In order to elucidate the correlation of paramagnetic defect centers with preexisting diamagnetic defects, the emphasis will be placed on comparison of the results of the ESR and vuv optical-absorption measurements, leading to the observation of the conversion of preexisting defects into paramagnetic defect species by 6.4 or 7.9 eV laser irradiation.

II. EXPERIMENTAL PROCEDURES

Samples used in the experiments are listed in Table I. They are classified in terms of oxygen stoichiometry and OH content. Samples OD1 and OD2 are of oxygen-deficient type, which contain neutral oxygen vacancies.[11] Sample OS is an oxygen-surplus-type silica, which contains excess oxygen either in the form of peroxy linkage or interstitial molecular oxygen.[13] Samples OD1 and OS were manufactured by the plasma method and OD2 by chemical vapor deposition (CVD)-soot remelting. These samples contain OH groups of less than a few ppm. Sample OH is a high-OH silica produced by flame hydrolysis, which contains OH groups of ≈ 1000 ppm. The dimension of the samples is a slab of $0.7 \times 2 \times 25$ mm^3 for ESR measurements or a mirror-polished plate with $\phi \approx 10$ mm and thickness of $t \approx 0.7$ mm for vuv absorption measurements.

Excimer-laser irradiation was carried out with a Lambda Physik LPX-105*i* excimer laser using Ar/F_2/He (193 nm, 6.4 eV) or F_2/He mixture (157 nm, 7.9 eV) as a lasing medium. Irradiation was carried out at room temperature in air for 6.4 eV photons and in N_2 atmosphere for 7.9 eV photons. Pulse energy was varied by changing operating conditions of the excimer laser, and the average pulse energy was estimated with a thermopile power meter (Scientech 38-2UV5). For reference, γ irradiation was carried out at room temperature with a ^{60}Co source at a dose rate of 85 Gy/hr to a total dose of 14.3 KGy.

The ESR measurement was performed using a JEOL RE2XG spectrometer operated at X-band frequency ($\nu \approx 9.25$ GHz) with a modulation amplitude of 0.063 mT. During the measurement, the sample in a quartz tube was kept at 77 K by immersing in liquid N_2. Microwave power was set at 1 μW for the detection of the E' centers and at 5 mW for the detection of oxygen hole centers (NBOHC and PR). The concentration of paramagnetic centers was determined by comparing results of double numerical integration of each ESR signature with that of the JEOL strong or weak pitch standard. The accuracy of the absolute concentration is $\approx \pm 50\%$, whereas that of the relative concentration is $\approx \pm 10\%$.

The vuv absorption measurement in the region of 6–8 eV was carried out with a 1-m Seya-Namioka-type monochromator using synchrotron radiation as a light source (0.38 GeV SR ring, Institute for Solid State Physics, The University of Tokyo, Tanashi, Tokyo).

III. RESULTS

A. Variation of ESR spectra with incident-photon energy

No ESR signal was detected in unirradiated samples. Figure 1 shows the ESR spectra of oxygen-deficient sample OD1 exposed to (a) 6.4 eV and(b) 7.9 eV laser photons. Both samples exhibit virtually identical spectra with only a signature of the E' center characterized by g values: $g_1 = 2.0018$, $g_2 = 2.0006$, and $g_3 = 2.0003$.[4,5] Similar spectra were obtained for the OD2.

Shown in Fig. 2 are the ESR spectra of oxygen-surplus sample OS exposed to (a) 6.4 eV and (b) 7.9 eV laser photons. In addition to the E' center, ESR signals due to the

TABLE I. Sample list.

Sample	Characteristics	Preparation method	Impurities (ppm) OH	Cl
OD1	oxygen deficient	Plasma CVD	0.75	3200
OD2	oxygen deficient	CVD soot remelting	ND	0.3
OS	oxygen surplus	Plasma CVD	0.46	320
OH	high-OH (stoichiometric[a])	Flame hydrolysis	1000	ND[b]

[a]No optical-absorption bands associated with oxygen vacancy or peroxy linkage.
[b]ND, not detected.

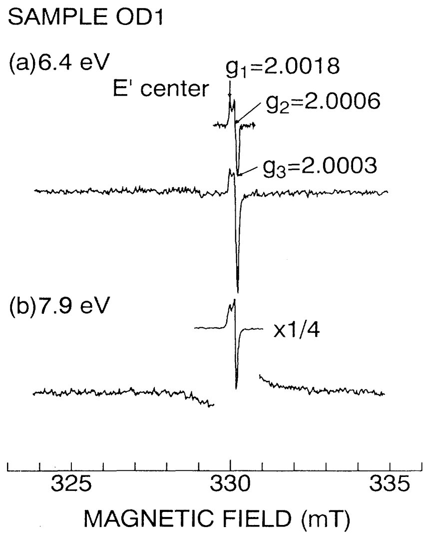

FIG. 1. ESR spectra of oxygen-deficient type silica OD1 exposed to (a) 6.4 eV (1.9×10^3 J/cm^2, 30 Hz) and (b) 7.9 eV (90 J/cm^2, 50 Hz) lasers. Spectra were recorded at X band and 77 K.

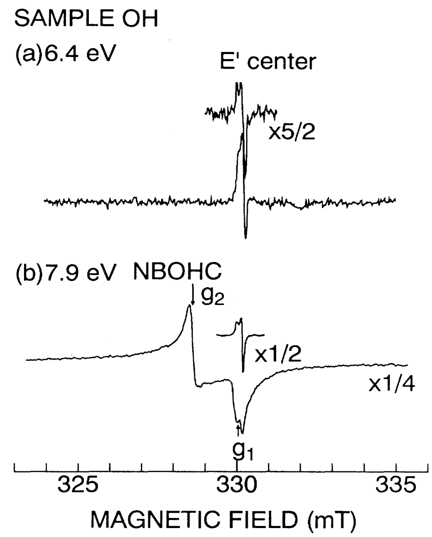

FIG. 3. ESR spectra of high-OH-type silica OH exposed to (a) 6.4 eV (1.9×10^3 J/cm^2, 30 Hz) and (b) 7.9 eV (90 J/cm^2, 50 Hz) lasers. Spectra were recorded at X band and 77 K.

NBOHC at $g_1=2.0015$ and $g_2=2.0099$ can be observed after exposure to either 6.4 or 7.9 eV photons.[4,5] The g_3 component at $g=2.078$ of the NBOHC is too broad to be detected in these spectra. Three features, each located at $g=2.0018$, $g=2.0079$, and $g=2.025$ are observed in the spectra of the sample irradiated by 7.9 eV photons. The features at $g_1=2.0018$ and $g_2=2.0079$ are part of the spectrum of PR's.[4,5] Although not shown in Fig. 2(b), a shoulder peak corresponding to the g_3 component at $g=2.067$ of the PR was observed at lower magnetic field. The other signature at $g=2.025$ is $m_I=\frac{1}{2}$ component of a four-line hyperfine spectrum, which was identified to be ClO_2 radicals (see Ref. 23).

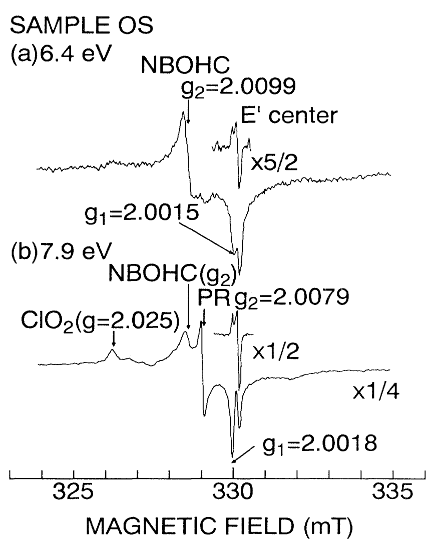

FIG. 2. ESR spectra of oxygen-surplus type silica OS exposed to (a) 6.4 eV (1.9×10^3 J/cm^2, 30 Hz) and (b) 7.9 eV (90 J/cm^2, 50 Hz) lasers. Spectra were recorded at X band and 77 K. A feature at $g\approx2.025$ in (b) corresponds to $m_I=\frac{1}{2}$ component of a four-line hyperfine spectrum of ClO_2 radicals (see also Ref. 23).

Figure 3 shows the ESR spectra of high-OH sample OH exposed to (a) 6.4 eV and (b) 7.9 eV laser photons. The E' centers are observable in sample OH exposed to either 6.4 or 7.9 eV photons. Curiously, the NBOHC's are dominantly observed when exposed to 7.9 eV photons, as shown in Fig. 3(b).

Note that when compared with the sharp g_2 peak at $g\approx2.01$ of the NBOHC's in Fig. 3(b) for the 7.9 eV irradiated sample OH, the corresponding peak in Fig. 2(a) for the 6.4 eV irradiated sample OS, appears to be somewhat broader at the bottom. Such broadening is more evident in Fig. 2(b) for the 7.9 eV irradiated sample OS. Therefore, there are undoubtedly some components superimposed on the "pure" g_2 peak of NBOHC's in oxygen-surplus sample OS. This will be discussed in detail in Sec. IV E.

Defect species and concentrations observed in these samples are summarized in Table II.

B. Dependence of defect concentration on laser fluence

Shown in Figs. 4(a) and 4(b) are the concentrations of the E' centers and NBOHC's plotted as a function of 6.4 eV laser fluence, respectively. The repetition rate and pulse energy were held constant (30 Hz, 35 mJ/cm^2 per pulse). The E' concentration in the low-OH samples OD1 and OS increases linearly with the fluence, while high-OH sample OH shows an immediate saturation followed by a gradual decay. Linear growth in the concentration of the NBOHC's is observed in the sample OS, as shown in Fig. 4(b).

TABLE II. Defect species and their concentration induced by 6.4 eV photons (fluence: 1.8×10^3 J/cm^2), 7.9 eV photons (fluence: 1.5×10^2 J/cm^2), and ^{60}Co γ rays (total absorbed dose: 1.4×10^4 Gy).

	Concentration (10^{14} cm^{-3})								
	Oxygen deficient (OD1)			Oxygen surplus (OS)			High-OH (OH)		
Radiation	E'	NBOHC	PR	E'	NBOHC	PR	E'	NBOHC	PR
6.4 eV	6.8	ND[a]	ND	11	180	ND	5.7	ND	ND
7.9 eV	120	ND	ND	150	D[b]	250	26	350	ND
γ rays	76	ND	ND	27	43	6.1	7.2	20	ND

[a]ND, not detected.

[b]D, detected but it was impossible to determine the absolute concentration due to the interference with strong signatures of PR and impurity-related radicals (see text).

Shown in Figs. 5(a) and 5(b) are the concentrations of the E' centers, NBOHC's, and PR's plotted as a function of 7.9 eV laser fluence (50 Hz, 3 mJ/cm^2). Saturation components are dominant in growth curves of the E' centers in the samples OD1, OS, and OH. For all samples, the E' concentration is one order of magnitude higher than the case of 6.4 eV photons. Peroxy radicals in the oxygen-surplus sample OS exhibits a monotonic growth over the whole range of laser fluence. A linear increase in the NBOHC concentration can be seen in the high-OH sample OH, followed by a saturation component.

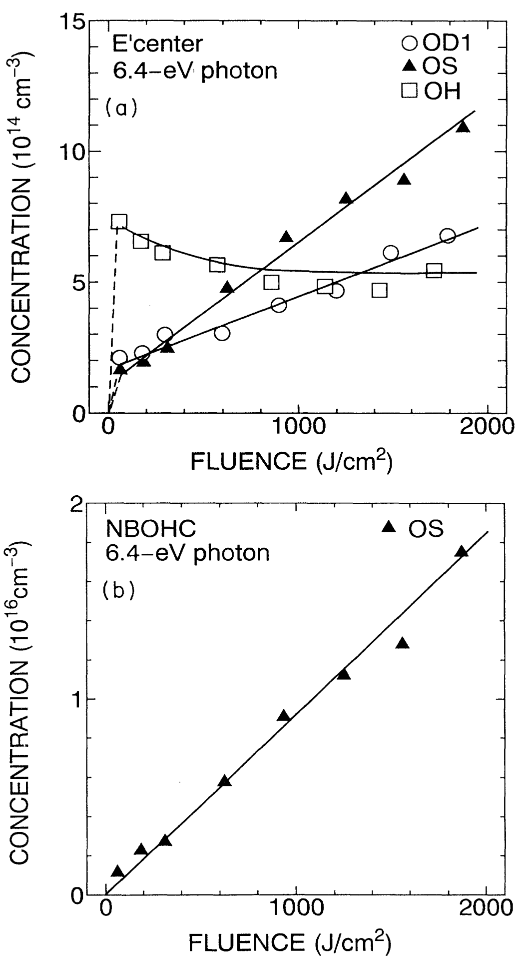

FIG. 4. Concentrations of (a) E' centers and (b) NBOHC's induced by a 6.4 eV laser as a function of laser fluence (○ OD1, (▲ OS, and □ OH). Pulse energy (35 mJ/cm^2) and repetition rate (30 Hz) were held constant.

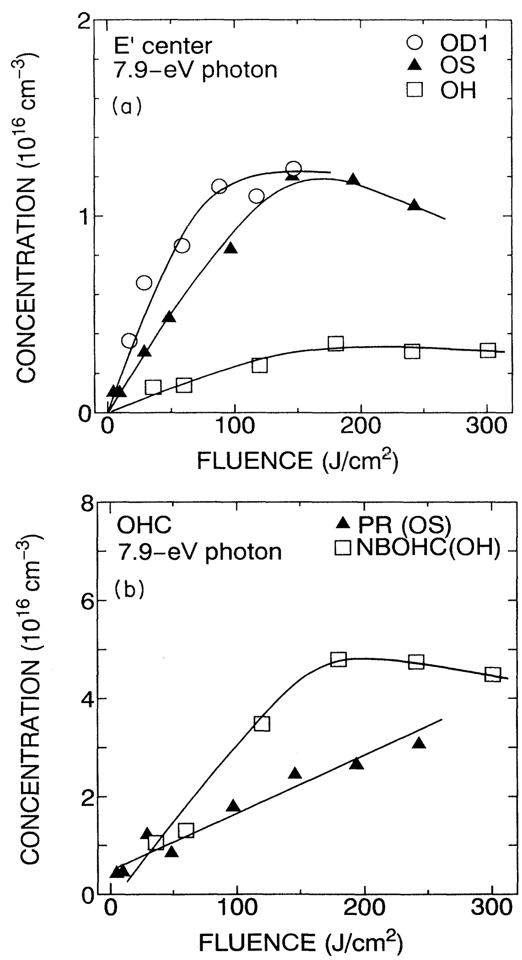

FIG. 5. Concentrations of (a) E' centers and (b) OHC's (PR's and NBOHC's) induced by a 7.9-eV laser as a function of laser fluence (○ OD1, (▲ OS, and □ OH). Pulse energy (3 mJ/cm^2) and repetition rate (50 Hz) were held constant.

C. Pulse-energy dependence of defect concentration

Shown in Fig. 6 is the concentration of the paramagnetic defects induced by 6.4 or 7.9 eV photons in (a) OD1, (b) OS, and (c) OH as a function of pulse energy. The repetition rate and irradiation time were held constant (30 Hz and 10 min for 6.4 eV photons, and 50 Hz and 10 min for 7.9 eV photons). In the low-OH samples OD1 and OS, the concentrations of the E' centers, NBOHC's, and PR's increase with the square of 6.4 or 7.9 eV laser-pulse energy, as shown in Figs. 6(a) and 6(b), where a log-log plot of the pulse energy versus the defect concentration gives a slope of 2. Although the slopes of the pulse-energy dependence of the E' center and NBOHC are ill defined due to the scattered data points in the high-OH sample OH exposed to 7.9 eV photons, superlinear features presumably due to two-photon processes, can be seen at pulse energies more than 1 mJ/cm^2. At a lower pulse-energy region, the concentrations of the E' centers and NBOHC's appear to increase with a slope of 1, suggesting a linear dependence of the defect concentration on the pulse energy.

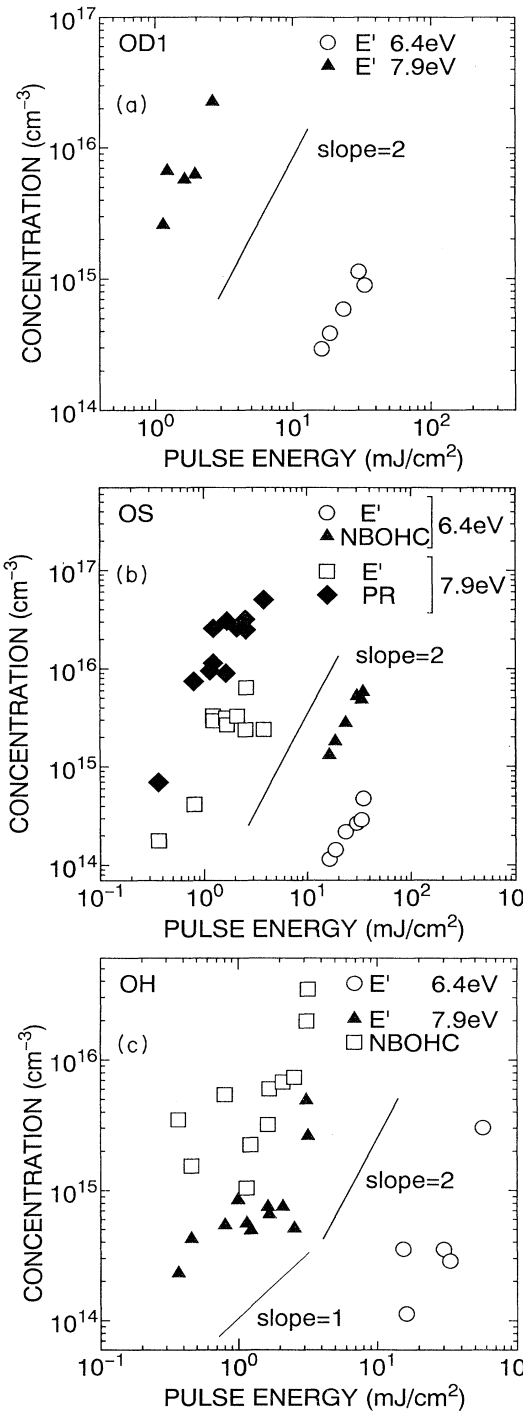

FIG. 6. Concentrations of paramagnetic centers induced by 6.4 eV (30 Hz, 10 min) or 7.9 eV photons (50 Hz, 10 min) in (a) oxygen-deficient silica OD1, (b) oxygen-surplus silica OS, and (c) high-OH silica OH as a function of pulse energy.

D. Vacuum-ultraviolet absorption spectra of unirradiated and irradiated silicas

Shown in Fig. 7 are the vuv absorption spectra of unirradiated samples OD1, OD2, OS, and OH. An absorption band is observed at 7.6 eV in oxygen-deficient samples OD1 and OD2, though the one in OD1 is so intense that the peak is driven off the scale. Oxygen-surplus sample OS exhibits an absorption tail from 7 to 8 eV. High-OH sample OH exhibits an absorption tail above 7.5 eV.

Figure 8 shows the change in absorption spectra of (a) OD2, (b) OS, and (c) OH induced by 6.4 or 7.9 eV laser irradiation. They were obtained by subtracting the spectra before irradiation from those after irradiation. Note that instead of using the sample OD1, the spectrum of the sample OD2 was chosen, since the 7.6-eV band in OD2 is moderate enough to see the change induced by irradiation. Oxygen-deficient sample OD2 shows a decrease of the 7.6-eV band and an increase of the background around 7 eV after exposed to 6.4 eV photons. Curiously, only in the case of the exposure to 7.9 eV photons, we observed an increase at 7.3 eV and a decrease at 7.9 eV. When exposed to 7.9 eV photons, oxygen-surplus

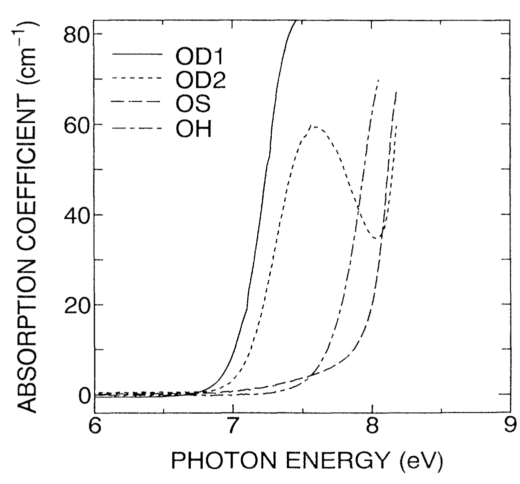

FIG. 7. Vacuum-ultraviolet absorption spectra of unirradiated silica glasses: oxygen-deficient silica OD1 and 2, oxygen-surplus silica OS, and high-OH silica OH.

sample OS exhibits a decrease of the broad absorption band from 7 to 8 eV, which has a valley at 7.9 eV. High-OH sample OH shows a decrease of tail above 7.5 eV only when exposed to 7.9 eV photons.

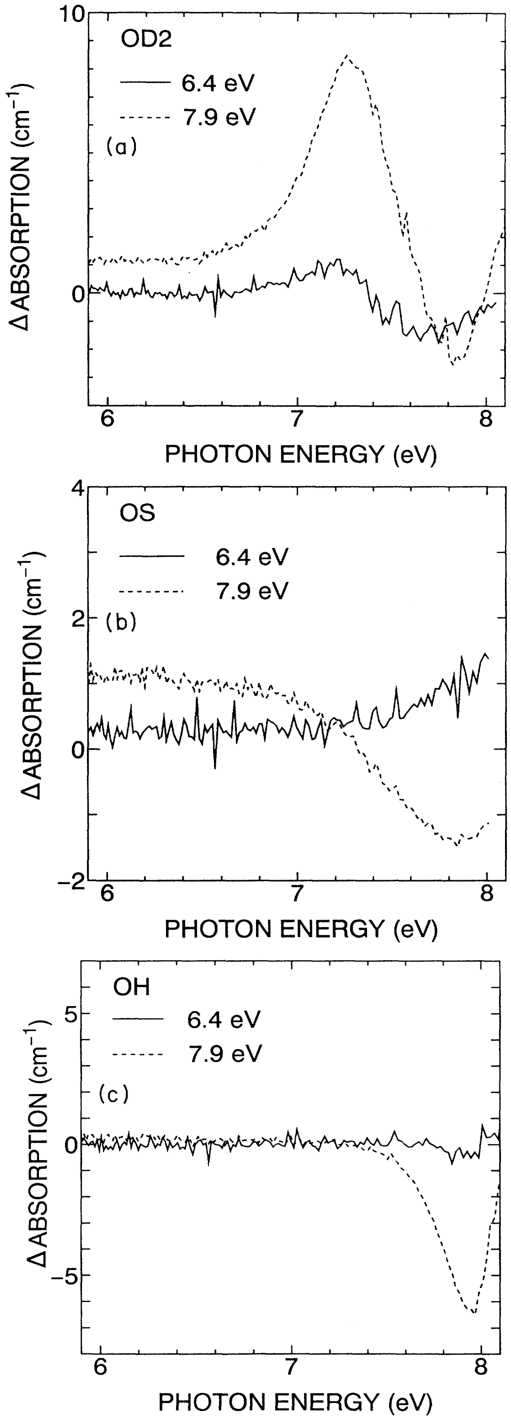

FIG. 8. Changes in vuv spectra of (a) oxygen-deficient silica OD2, (b) oxygen-surplus silica OS, and (c) high-OH silica OH induced by 6.4 eV (solid curves, 30 Hz, fluence: 1.9×10^3 J/cm^2) and 7.9 eV laser (broken curves, 50 Hz, fluence: 2.3×10^2 J/cm^2).

IV. DISCUSSION

The following discussion comprises five subsections from Sec. IV A–Sec. IV E. First, discussed in Sec. IV A is variation of laser-induced paramagnetic defects with incident-photon energy, laser fluence, and pulse energy. In Sec. IV B, preexisting defects introduced during manufacture are discussed on the basis of the vuv absorption spectra. Then in Sec. IV C, correlation between the induced paramagnetic defects and preexisting defects is discussed. Specific defect formation reactions are discussed for E' centers, NBOHC's, and PR's. In Sec. IV D, defect formation processes are discussed on the basis of an energy diagram of precursor defects. Finally, in Sec. IV E, comparison with other experiments is made.

A. Induced paramagnetic defects

One of the interesting features is the variation in the ESR spectra in Figs. 1–3 and growth curves in Figs. 4 and 5, with incident laser-photon energy. As shown in Table II, induced defect species and their concentrations are found to be sensitive to the incident laser-photon energy, as well as to the OH concentration and oxygen stoichiometry. The dependence on the type of silica suggests that precursors of the induced paramagnetic species are preexisting defects introduced during manufacture. Thus, the dependence on the incident-photon energy can be accounted for by the variation of defect formation reactions. We also note in Figs. 4 and 5 that the growth of paramagnetic defects as a function of laser fluence varies again with both the OH concentration and stoichiometry. As already mentioned, the growth curves of paramagnetic defects seem to comprise three regions, i.e., linear growth, saturation, or decay component, depending on the types of samples. This also reflects the variation in the defect formation reactions. Kinetics of defect formations should be discussed taking into account the secondary reactions involving the diffusion of mobile species such as atomic hydrogen and oxygen, but won't be discussed in detail here.

Another important result is the pulse-energy dependence of induced paramagnetic defects shown in Fig. 6. It is shown from the square pulse-energy dependence that a two-photon absorption process is involved in the formation of the E' centers, NBOHC's, and PR's both for the cases of 6.4 and 7.9 eV photons. These results are reasonable in view of the fact that the band gap of a-SiO_2 (≈ 9 eV) (Ref. 15) is higher than the one-photon energy but lower than the two-photon energy of either the 6.4 or 7.9 eV photon. This means that the defect reactions follow the band-to-band electronic excitation through two-photon absorption.

B. Preexisting diamagnetic defects

As shown in Fig. 7, several absorption bands are observed at 7–8 eV in the vuv spectra of unirradiated silicas. Since these unirradiated silicas exhibit no paramagnetism, diamagnetic defects are responsible for these vuv absorption bands. Thus, possible precursors for laser-induced paramagnetic defects are such diamagnetic defects introduced during manufacture.

The intense absorption band at 7.6 eV can be seen in oxygen-deficient silicas OD1 and OD2. Although there still remains a debate over the structural models for oxygen-deficient center,[5] it has been generally regarded that the 7.6-eV band arises from oxygen vacancy denoted as $\equiv$Si—Si$\equiv$.[5,9,11] This model is supported by the results of *ab initio* molecular-orbital calculation,[11] or by analogy with an absorption spectrum of the Si_2H_6 molecule.[9] The concentrations of the $\equiv$Si—Si$\equiv$ structure in samples OD1 and OD2 are estimated to be $>10^{18}$ cm^{-3} and 7×10^{17} cm^{-3}, respectively, using an absorption cross section of $\sigma=8\times10^{-17}$ cm^2 reported by Imai *et al.*[9]

The absorption tail observed at 7–8 eV in oxygen-surplus type silica OS has been assigned to either peroxy linkage ($\equiv$Si—O—O—Si$\equiv$) or dissolved O_2.[18,24] The former assignment is based on theoretical calculations[25,26] and experimental results of H_2 treatment.[18] The latter assignment is, on the other hand, based on the similarity with Schumann-Runge band due to O_2 molecule.[24] Since the peroxy linkages and O_2 molecules coexist in the oxygen-surplus sample,[13] both of these two absorption bands can overlap in the region of 7–8 eV. Since these two bands cannot be isolated in the vuv spectrum, we will consider both models for the 7–8 eV band in the following discussion.

The absorption band above 7.5 eV in high-OH sample OH has been attributed to Si—OH bonds, with a fairly well-established correlation between the absorption intensity and the hydroxyl concentration.[18] Since the samples contain fairly large concentrations of hydroxyl or chlorine, impurity-related defects such as Si-H and Si-Cl are possibly present. Although they can give rise to optical absorption above 8 eV,[18,24] both are unobservable in the vuv spectra of Fig. 7. This is due to the interference with the intense absorption edge of a-SiO_2.

C. Correlation between induced paramagnetic defects and preexisting diamagnetic defects

1. *E′ center*

Oxygen vacancy ($\equiv$Si—Si$\equiv$) has long been accepted as one of the precursors for the E' centers. As predicted by the theory of Feigl, Fowler, and Yip,[27] hole trapping at the site of the oxygen vacancy results in the formation of the E' center, or positively charged oxygen vacancy:[3]

$$\equiv\mathrm{Si}\text{—}\mathrm{Si}\equiv\ \rightarrow\ \equiv\mathrm{Si}\cdot+{}^{+}\mathrm{Si}\equiv+e^{-}\ . \tag{1}$$

As shown in Fig. 8(a), a decrease of the 7.6-eV band is observed in oxygen-deficient sample OD2 in the case of 6.4 eV photons. Also in the case of 7.9 eV photons, a decrease of the 7.6-eV band is seen at 7.6–8 eV though an increase is observed at the lower energy region.[28] These results support the conversion of the oxygen vacancy into the E' center, as expressed by the reaction of Eq. (1).

The mechanism of Eq. (1) can be only applicable to oxygen-deficient-type silicas, in which the 7.6-eV band is observed. In the case of high-OH silica, $\equiv$Si—H bond has been considered as one of the E' precursors:[18,21]

$$\equiv\mathrm{Si}\text{—}\mathrm{H}\rightarrow\ \equiv\mathrm{Si}\cdot+\cdot\mathrm{H}\ . \tag{2}$$

Still, neither Eq. (1) nor (2) explains the creation of the E' centers in the low-OH oxygen-surplus silica OS, whose concentration is comparable with those in samples OD1 and OH. Assuming that chlorine of 370 ppm in the sample is all incorporated in the form of Si—Cl bonds, the formation of E' centers in sample OS can be attributed to the fission of the Si—Cl bonds:[23,29]

$$\equiv\mathrm{Si}\text{—}\mathrm{Cl}\rightarrow\ \equiv\mathrm{Si}\cdot+\cdot\mathrm{Cl}\ . \tag{3}$$

The atomic chlorine ($\cdot$Cl) in the right-hand side of Eq. (3) has been reported to form ClO_x ($x=2,3$) radicals as a result of the reaction with excess oxygen.[23] A part of the spectrum of ClO_2 radicals can be seen in Fig. 2(b). The decay of the absorption band associated with Si—H and Si—Cl bonds is expected for the mechanisms of Eqs. (2) and (3), respectively, in harmony with the annihilation of the precursors in the left-hand sides of these equations. Unfortunately, this could not be confirmed due to the overlap with intense absorption edge above 8 eV.

2. *NBOHC's*

The NBOHC's are observable in the oxygen-surplus silica OS for the case of either 6.4 or 7.9 eV photons. As we discussed about the vuv spectrum, two forms of excess oxygen, peroxy linkage ($\equiv$Si—O—O—Si$\equiv$) and O_2 molecule, are suggested to preexist in sample OS. Peroxy linkage has been reported to be a candidate for the precursor in oxygen-surplus sample OS:[21]

$$\equiv\mathrm{Si}\text{—}\mathrm{O}\text{—}\mathrm{O}\text{—}\mathrm{Si}\equiv\ \rightarrow\ \equiv\mathrm{Si}\text{—}\mathrm{O}\cdot+\cdot\mathrm{O}\text{—}\mathrm{Si}\equiv\ . \tag{4}$$

Another possible reaction involves the production of atomic oxygen by the dissociation of the O_2 molecule and its subsequent trapping at the E' center produced by Eq. (3):[23,24]

$$O_2\rightarrow2O \tag{5}$$

and

$$\equiv\mathrm{Si}\cdot+\mathrm{O}\rightarrow\ \equiv\mathrm{Si}\text{—}\mathrm{O}\cdot\ . \tag{6}$$

The photochemical reaction of Eq. (5) has been reported to occur by excitation with photon energy above 5.1 eV.[24] As shown in Fig. 8(b), however, vuv spectral change is scarcely observed in the case of 6.4 eV photons. The concentration of the induced NBOHC's (1.8×10^{16} cm^{-3}) in the sample OS is one order of magnitude smaller than those of precursors (e.g., peroxy linkages: 7×10^{17} cm^{-3} from Ref. 13; O_2: $\approx10^{17}$ cm^{-3} from Ref. 24). The resulting optical-absorption change might be below the detection limit. By contrast, a decrease of the 7–8 eV tail absorption can be clearly seen in Fig. 8(b) for the case of 7.9 eV photons. This result supports the reaction of Eq. (4) or those of Eqs. (5) and (6).

Nonbridging oxygen hole centers are also observable in high-OH silica OH only after exposure to 7.9 eV photons. The formation of the NBOHC's in the high-OH silica has been attributed to the rupture of Si—OH bonds which are abundant (≈1000 ppm) in the sample:[30]

$$\equiv \text{Si—OH} \rightarrow \equiv \text{Si—O}\cdot + \cdot\text{H} \ . \tag{7}$$

In fact, as shown in Fig. 8(c), sample OH exhibits a sharp decrease at 8 eV only when exposed to 7.9 eV photons. Therefore, this can be attributed to the transformation of Si—OH bonds into NBOHC's according to Eq. (7). In this case, we can estimate the concentrations of both the decreased Si—OH bonds and induced NBOHC's. The concentration of the decreased Si—OH bonds is estimated to be $\approx 4\times10^{19}$ cm^{-3} using an absorption cross section of $\sigma = 1.1\times10^{-19}$ cm^2 for Si—OH at 7.8 eV.[31] Curiously, this value is three orders of magnitude higher than that of the NBOHC's [$\approx 5\times10^{16}$ cm^{-3} estimated from Fig. 5(b) for the 7.9 eV laser fluence of 2.3×10^2 J/cm^2]. This suggests that most of the induced NBOHC's become ESR-inactive by trapping electrons or holes. For example, it might be reasonable to assume formation of such a negatively charged nonbridging oxygen ($\equiv$Si—O^-) as a result of electron trapping, in view of the fact that the E' center can be created by ejecting an electron through the reaction of Eq. (1).

3. *Peroxy radical*

Peroxy radicals are observed in oxygen-surplus silica only when exposed to 7.9 eV photons, while not when exposed to 6.4 eV photons. It has been thought that PR's can be created by hole trapping on a peroxy linkage:[3]

$$\equiv \text{Si—O—O—Si} \equiv \rightarrow \equiv \text{Si—O—O}\cdot + {}^{+}\text{Si}\equiv + e^- \ , \tag{8}$$

or by the reaction of an interstitial O_2 molecule with an E' center:[32,33]

$$\equiv \text{Si} + \text{O}_2 \rightarrow \equiv \text{Si—O—O}\cdot \ . \tag{9}$$

Since the reaction of Eq. (9) is a diffusion-limited reaction which can be thermally activated at temperatures above 200 °C,[32] it could be prohibited in the present experimental condition. On the other hand, atomic oxygen induced as a result of the photochemical reaction of Eq. (5) can easily diffuse at room temperature and then react with an E' center:[23]

$$\equiv \text{Si}\cdot + 2\text{O} \rightarrow \equiv \text{Si—O—O}\cdot \ . \tag{10}$$

Both mechanisms of Eqs. (8) and (10) are possible candidates for the production of the PR's in sample OS. That the 7–8 eV band is decreased after exposure to 7.9 eV photons is in good agreement with the mechanisms of both Eqs. (8) and (10) for PR's.

Reactions discussed in Sec. IV C are summarized in Table III.

D. Photon-energy dependence of defect formation reactions

Next, we turn to the photon-energy dependence of defect formation reactions. First of all, it is instructive to discuss the band-to-band excitation induced by two-photon absorption of 6.4 and 7.9 eV photons. Shown in Fig. 9 is the schematic illustration of the energy diagram of defects in SiO_2 calculated by O'Reilly and Robertson.[25,26] The valence band (VB) comprises the upper and lower VB's, each corresponding to the oxygen nonbonding state and Si—O bonding state, respectively. The energy gap between the conduction band (CB) and the upper VB, and the one between the CB and the lower VB are estimated to be ≈ 9 and ≈ 14 eV, respectively. Therefore, two-photon excitation by 6.4 eV photons can excite an electron from the *upper* VB to the CB, while two-photon excitation by 7.9 eV photons can excite an electron from the *lower* VB to the CB.

TABLE III. Paramagnetic defect centers induced by 6.4 and 7.9 eV photons, and by γ rays, their possible precursors, and occurrence.

Paramagnetic defect center	Sample	Precursor: Species	Precursor: Density (cm^{-3})	Occurrence[a]: 6.4 eV	Occurrence[a]: 7.9 eV	Occurrence[a]: γ rays
	OD1	$\equiv$Si—Si$\equiv$	$>10^{18}$ [b]	yes	yes	yes
	OD2	$\equiv$Si—Si$\equiv$	7×10^{17} [b]	yes	yes	yes
E' ($\equiv$Si$\cdot$)	OS	$\equiv$Si—Cl	7×10^{18} [c]			
	OH	$\equiv$Si—H		yes	yes	yes
NBOHC ($\equiv$Si—O$\cdot$)	OS	$\equiv$Si—O—O—Si$\equiv$	7×10^{17} [d]	yes	yes	yes
	OS	O_2 ($\rightarrow$2O) $\equiv$Si$\cdot$+O	$\approx10^{17}$ [e]	no	yes	
	OH	$\equiv$Si—OH	8×10^{19} [f]	no	yes	yes
PR ($\equiv$Si—O—O$\cdot$)	OS	$\equiv$Si—O—O—Si$\equiv$	7×10^{17} [d]	yes	yes	yes
	OS	O_2 ($\rightarrow$2O) $\equiv$Si$\cdot$+2O	$\approx10^{17}$ [e]	no	yes	

[a]Possibility of the reaction occurrence (see text in Sec. IV D).
[b]Estimated using absorption cross section of $\sigma = 8\times10^{-17}$ cm^2 for $\equiv$Si—Si$\equiv$ (Ref. 9).
[c]Estimated by assuming that all chlorine exists in the form of Si—Cl.
[d]Reference 13.
[e]Reference 24.
[f]Estimated from IR absorption intensity at 3650 cm^{-1}.

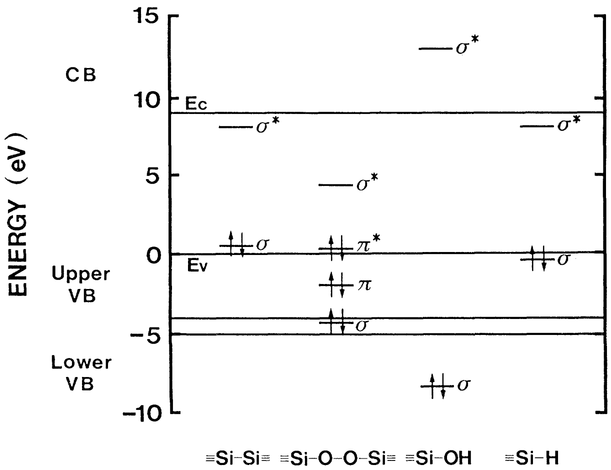

FIG. 9. The energy diagram of various preexisting defects in SiO_2 calculated by O'Reilly and Robertson (after Refs. 25 and 26) reproduced from Ref. 21. The upper valence band at -4–0 eV comprises nonbonding states and the lower valence band below -5 eV comprises Si—O bonding states.

Since defect formation reactions follow the formation of an electron-hole (*e-h*) pair through the band-to-band excitation, there are two possible mechanisms by which paramagnetic defects are created from preexisting precursors: electron rearrangement [such as Eqs. (1) and (8)], and radiolytic reactions [such as Eqs. (2)–(5) and (7)]. Therefore, defect reactions critically depend on the location of energy levels of precursor defects in the band gap of a-SiO_2. Using the energy diagram shown in Fig. 9, we can discuss the occurrence of specific defect reactions.

Occurrence of the defect formation reactions is summarized in Table III. In the case of electron rearrangement, for example, since the ≡Si—Si≡ bond has a filled bonding state at ≈ 0.5 eV above the E_v, the occurrence of the reaction of Eq. (1) is expected through trapping of a hole in the *upper* VB at the site of the oxygen vacancy. If we suppose that the O—Si bonding state of peroxy linkage (not reported in the literature) lies within the O—Si bonding states of the normal Si—O—Si network (i.e., lower VB), creation of a hole in the *lower* VB is required for the hole trapping at the O—Si bond of peroxy linkage [Eq. (8)]. Therefore, while the occurrence of the reaction of Eq. (1) is possible in the case of either the 6.4 or 7.9 eV photon, the occurrence of the reaction of Eq. (8) is possible only in the case of 7.9 eV photon.

On the other hand, the occurrence of the radiolytic reactions of Eqs. (2)–(4) and (7) should be determined by the quantitative relation between defect formation energy [i.e., the energy difference between bonding (σ) and antibonding (σ^*) states, $E_{\sigma-\sigma^*}$] of precursor defects and the energy released by the relaxation of an *e-h* pair. From the energy diagram, the value of the $E_{\sigma-\sigma^*}$ is estimated to be ≈ 8–9 eV for the ≡Si—H and O—O bonds. The value of $E_{\sigma-\sigma^*}$ of about 20 eV for the O—H bond in Fig. 9 should be extended down to about ≈ 15 eV, when the broad density of states of Si—OH is taken into account.[25] Based on this argument, energy released by the decay of an *e-h* pair created by two-photon absorption of 6.4 eV light is sufficient to induce rupture of the ≡Si—H [Eq. (2)] and O—O bonds [Eq. (4)], while it is insufficient to induce rupture of the O—H bond [Eq. (7)]. It is considered that the rupture of the O—H is possible only when two-photon excitation by 7.9 eV photons occurs.

The formations of NBOHC's in Eq. (6) and PR's in Eq. (10) assume the generation of atomic oxygen by Eq. (5). Thus, yields of these reactions should be subject to photon-energy dependence of the atomic oxygen yield. In fact, the absorption coefficient of O_2 at 7.9 eV is reported to be about four orders of magnitude higher than at 6.4 eV.[34] Therefore, in the case of the 7.9 eV photon, the generation of the NBOHC's and PR's through Eqs. (6) and (10), respectively, is expected to be several orders of magnitude higher than in the case of the 6.4 eV photon. Actually, this is in good accord with the photon-energy dependence of the PR's of sample OS, as shown in Table II.

As discussed above, photon-energy dependence can be understood in terms of the difference in the excitation process between 6.4 and 7.9 eV laser irradiations. Therefore, qualitative agreement between the results of 7.9 eV photons and γ rays is reasonable, since γ irradiation is expected to cause excitation of electrons from the *lower* VB as in the case of 7.9 eV photons.

E. Comparison with other experiments

The results of the two-photon process are in good accord with the results reported for low-OH oxygen-deficient silicas by Imai, Arai, and co-workers,[17,18] and high-OH silica (Suprasil) by Tsai, Griscom, and Friebele[19,35] in the case of 6.4 eV photons. While the pulse-energy dependence for the 7.9 eV induced defects has never been reported so far to our knowledge, present results show that the two-photon process is the rate-limiting step in the case of 7.9 eV photons.

Next, we turn to the ESR spectra and their interpretation. The results of oxygen-deficient sample OD are in good agreement with those reported by Imai and coworkers.[17,18] The spectra of oxygen-surplus sample OS in Figs. 2(a) and 2(b) are quite similar to those reported by Stathis and Kastner[14] for commercially available Suprasil W. It was argued in Ref. 14 that the signal at $g \approx 2.01$ may consist of several superimposed components due to unknown impurities. The component at $g \approx 2.01$ in Fig. 2(b) is, in fact, somewhat broader than those seen in both Figs. 2(a) and 3(b). Furthermore, such broadening appears in concert with the appearance of a feature at $g \approx 2.025$ due to ClO_2 radicals, as shown in Figs. 2(a) and 2(b). Thus, our tentative interpretation is that such broadening is due to the presence of the superimposed components associated with both impurity chlorine and excess oxygen.

The results of 7.9 eV excitation of the OH sample are in marked conflict with those reported in Ref. 14. A three-line spectrum dominates for high-OH silica (Suprasil) in the spectrum in Ref. 14, while the E' centers and NBOHC's dominate in Fig. 3(b) for sample OH. The three-line spectrum was first attributed to the hyperfine interaction of an unpaired spin with nitrogen ($I=1$ nucleus) by Stathis and Kastner[14] and later has been characterized by Tsai, Griscom, and Friebele[36] as an unpaired electron occupying an sp^n hybrid orbital of the nitrogen and a neighboring silicon. According to Ref. 36, sample-to-sample variation was observed in the appearance of the nitrogen centers in different lots of Suprasil 1. Thus, the discrepancy can be attributed to the fact that our high-OH sample contains much less impurity nitrogen in contrast to the high-OH sample (Suprasil) used by Stathis and Kastner. Another possible reason for the discrepancy is that our ESR measurements at 77 K afforded us higher sensitivity for the detection of the NBOHC's and E' center in concentrations as low as $\approx 10^{15}-10^{16}$ cm^{-3} than in the measurements at room temperature performed in Ref. 14.

V. SUMMARY

We have performed ESR and vuv absorption measurements on a series of silica glasses unirradiated and those irradiated by 6.4 or 7.9 eV photons from excimer lasers. The results of the ESR measurements show that defect species and their concentrations are strongly influenced by both the manufacturing process and incident-photon energy. It is shown that defect species induced by γ rays are in a good agreement with those induced by 7.9 eV photons. The influence of the manufacturing methods and conditions can be explained by variation in preexisting defect species. The defect formation process can be understood in terms of the creation of an *e-h* pair as a result of two-photon absorption, and subsequent hole trapping or recombination of *e-h* pair at the site of preexisting defects, leading to the formation of paramagnetic defect centers. The photon-energy dependence is explained in terms of the energy levels of preexisting defects. The changes in the vuv spectra induced by 6.4 or 7.9 eV photons are also examined in order to elucidate correlations of preexisting defects with laser-induced defects. We observed the decrease of the 7.6 eV band, 7–8 eV band, and absorption tail above 7.5 eV, associated with the annihilation of oxygen vacancies, excess oxygen (peroxy linkages or molecular oxygen), and hydroxyls, respectively. Comparison of the results of the vuv absorption measurements with those of the ESR study has given direct evidence for the conversion of these preexisting defects into E' centers, NBOHC's, and PR's under 6.4 or 7.9 eV laser irradiation.

ACKNOWLEDGMENTS

Some of the samples were provided by courtesy of Shin-Etsu Quartz Products Co., Ltd., and Shin-Etsu Chemical Co., Ltd. This work was partly supported by Grant-in-Aid for Scientific Research (No. 03452156) from the Ministry of Education, Science and Culture of Japan, by Izumi Science and Technology Foundation, by the foundation "Hattori-Hokokai," and by the 1991–92 Waseda University Annual Project. One of the authors (H.N.) acknowledges encouragement by Professor Kaya Nagasawa of the Shonan Institute of Technology. This work was performed using facilities of the Institute for Solid State Physics, the University of Tokyo. The authors acknowledge Dr. Masami Fujisawa for his technical advice.

*Present address: Department of Electrical Engineering, Tokyo Metropolitan University, 1,1-Chome, Minami-Osawa, Hachioji-City, Tokyo 192-03, Japan.

[1] D. L. Griscom, in *Proceedings of the Thirty-Third Frequency Control Symposium* (Electronic Industries Association, Washington, D.C., 1979), p. 98.

[2] D. L. Griscom, in *Radiation Effects of Optical Materials,* The Society of Photo-Optical Instrumentation Engineers Conference Proceedings, edited by P. W. Levy (SPIE, Bellingham, WA, 1985), Vol. 541, p. 38.

[3] D. L. Griscom, in *Defects in Glasses,* edited by F. L. Galeener, D. L. Griscom, and M. J. Weber, Materials Research Society Symposia Proceedings No. 61 (Materials Research Society, Pittsburgh, 1986), p. 213.

[4] D. L. Griscom, Rev. Solid State Sci. **4**, 565 (1990).

[5] D. L. Griscom, J. Ceram. Soc. Jpn. **99**, 923 (1991).

[6] R. A. Weeks, J. Appl. Phys. **27**, 1376 (1956).

[7] D. L. Griscom, Phys. Rev. B **40**, 4224 (1989).

[8] H. Imai, K. Arai, T. Saito, S. Ichimura, H. Nonaka, J. P. Vigouroux, H. Imagawa, H. Hosono, and Y. Abe, in *The Physics and Technology of Amorphous SiO_2,* edited by R. A. B. Devine (Plenum, New York, 1988), p. 153.

[9] H. Imai, K. Arai, H. Imagawa, H. Hosono, and Y. Abe, Phys. Rev. B **38**, 12 772 (1988); H. Hosono, Y. Abe, H. Imagawa, H. Imai, and K. Arai, *ibid.* **44**, 12 043 (1991).

[10] K. Nagasawa, Y. Hoshi, and Y. Ohki, Jpn. J. Appl. Phys. **26**, L554 (1987).

[11] R. Tohmon, H. Mizuno, Y. Ohki, K. Sasagane, K. Nagasawa, and Y. Hama, Phys. Rev. B **39**, 1337 (1989).

[12] K. Awazu, H. Kawazoe, and K. Muta, J. Appl. Phys. **69**, 4183 (1991).

[13] H. Nishikawa, R. Tohmon, Y. Ohki, K. Nagasawa, and Y. Hama, J. Appl. Phys. **65**, 4672 (1989).

[14] J. H. Stathis and M. A. Kastner, Phys. Rev. B **29**, 7079 (1984).

[15] T. H. DiStefano and D. E. Eastman, Solid State Commun. **9**, 2259 (1971).

[16] R. A. B. Devine, Ref. 3, p. 177.

[17] K. Arai, H. Imai, H. Hosono, Y. Abe, and H. Imagawa, Appl. Phys. Lett. **53**, 1981 (1988).

[18] H. Imai, K. Arai, H. Hosono, Y. Abe, T. Arai, and H. Imagawa, Phys. Rev. B **44**, 4812 (1991).

[19] T. E. Tsai, D. L. Griscom, and E. J. Friebele, Phys. Rev. Lett. **61**, 444 (1988).

[20] T. E. Tsai and D. L. Griscom, Phys. Rev. Lett. **67**, 2517 (1991).

[21] H. Nishikawa, R. Nakamura, R. Tohmon, Y. Sakurai, K. Nagasawa, and Y. Hama, Phys. Rev. B **41**, 7828 (1990).

[22] D. L. Staebler and C. W. Wronski, Appl. Phys. Lett. **31**, 292 (1977).

[23] H. Nishikawa, R. Nakamura, Y. Ohki, K. Nagasawa, and Y.

Hama, Phys. Rev. B **46**, 8073 (1992).
[24]K. Awazu and H. Kawazoe, J. Appl. Phys. **68**, 3584 (1990).
[25]E. P. O'Reilly and J. Robertson, Phys. Rev. B **27**, 3780 (1983).
[26]J. Robertson, Ref. 3, p. 91.
[27]F. J. Feigl, W. B. Fowler, and K. L. Yip, Solid State Commun. **14**, 225 (1974).
[28]Although the interpretation of the vuv spectral change induced by 7.9 eV photons cannot be straightforward, the result of 7.9 eV photons is virtually identical to that of 6.4 eV photons in that both exhibit the annihilation of the oxygen vacancies. Our tentative interpretation is that the 7.6 eV band grows as a result of creation of new oxygen vacancies, while a hole burning of the spectrum at 7.9 eV simultaneously occurs as a result of a selective photobleaching of a part of new or preexisting oxygen vacancies. This is consistent with the results of uv absorption showing the simultaneous increase of the 5.0-eV band due to oxygen vacancies [see H. Nishikawa, R. Nakamura, K. Nagasawa, Y. Ohki, and Y. Hama, in *Proceedings of the Third Symposium, International Symposium on Structural Imperfections in SiO_2-based Amorphous Materials,* edited by H. Kawazoe, H. Imagawa, and K. Arai, Transactions of The Materials Research Society of Japan, (MRS Japan, 1992), Vol. 8, p. 120].
[29]D. L. Griscom and E. J. Friebele, Phys. Rev. B **34**, 7524 (1986).
[30]M. Stapelbroek, D. L. Griscom, E. J. Friebele, and G. H. Sigel, Jr., J. Non-Cryst. Solids **32**, 313 (1979).
[31]K. Awazu, Ph.D. thesis, Tokyo Institute of Technology, 1991.
[32]A. H. Edwards and W. B. Fowler, Phys. Rev. B **26**, 6649 (1982).
[33]R. L. Pfeffer, Ref. 8, p. 181.
[34]D. H. Volman, in *Advances in Photochemistry,* edited by W. A. Noyes, Jr., G. S. Hammond, and J. N. Pitts, Jr. (Interscience, New York, 1963), Vol. 1, p. 44.
[35]T. E. Tsai, D. L. Griscom, and E. J. Friebele, in *Properties and Characteristics of Optical Glass,* The Society of Photo-Optical Instrumentation Engineers Conference Proceedings, edited by A. J. Marker (SPIE, Bellingham, WA, 1988), Vol. 970, p. 165.
[36]T. E. Tsai, D. L. Griscom, and E. J. Friebele, Phys. Rev. B **38**, 2140 (1988).